Syntheses, Structure, and Magnetic Properties of New Types of Cu(II), Co(II), and Mn(II) Organophosphonate Materials: Three-Dimensional Frameworks and a One-Dimensional Chain Motif

Deyuan Kong,[†] Yang Li,[‡] Xiang Ouyang,[†] Andrey V. Prosvirin,[†] Hanhua Zhao,[†] Joseph H. Ross, Jr.,[‡] Kim R. Dunbar,[†] and Abraham Clearfield*,[†]

Department of Chemistry, Texas A&M University, College Station, Texas, 77842, and Department of Physics, Texas A&M University, College Station, Texas, 77843

The hydrothermal syntheses, structures, and magnetic properties of the Cu(II), Co(II), and Mn(II) complexes with organophosphonic acid $H_2O_3PCH_2NH_2^+CH_2PO_3H^-$ are reported. Compound $Cu_3[NH_2(CH_2PO_3)_2]_2$ (**1**) crystallizes in the orthorhombic space group *Pbca*, with unit cell parameters $a = 9.4430(10)$ Å, $b = 9.3681(10)$ Å, $c = 16.0755(17)$ Å, $V = 1422.1(3)$ Å^3, and $Z = 4$. The X-ray crystallographic determination reveals copper ions in two different coordination environments that are bridged by one terminal oxygen atom to form a three-dimensional framework of corner-sharing layers. Antiferromagnetic coupling between the two types of Cu units in **1** was observed at 15 K, followed by ferromagnetic ordering at 9 K. Compound $Co_3[NH_2(CH_2PO_3)_2]_2$ (**2**) crystallizes in the orthorhombic space group $P2_12_12$ with unit cell parameters $a = 10.7346(8)$ Å, $b = 13.3704(10)$ Å, $c = 5.3699(4)$ Å, $V = 770.72(10)$ Å^3, and $Z = 2$. All Co(II) ions are in a tetrahedral environment with both ends of the ligand bound via O atoms to adjacent Co(II) ions, thus creating tetranuclear 16-membered rings. Compound $Mn\{[NH_2(CH_2PO_3H)_2]_2(H_2O)_2\}$ (**3**) crystallizes in the monoclinic space group $P2_1/n$, with unit cell parameters $a = 7.3668(11)$ Å, $b = 8.1540(12)$ Å, $c = 14.090(2)$ Å, $\beta = 103.935(2)°$, $V = 821.4(2)$ Å^3, and $Z = 2$. Four phosphate oxygen atoms and two water molecules are coordinated to the mononuclear octahedral Mn(II) ions. The amino groups are protonated and therefore do not coordinate to Mn(II). Compound **3** features a one-dimensional chain architecture stitched together by hydrogen bonds.

Introduction

Metal phosphonates have potential applications in the areas of catalysis, ion exchange, proton conductivity, intercalation chemistry, photochemistry, and chemistry of materials.[1] The majority of these phosphonates are layered species with the metal octahedra bridged by phosphonic acid tetrahedra to form two-dimensional layers that are separated by hydrophobic regions of the organic moieties. Although the poor crystallinity of these compounds renders their structural analysis a difficult task, the hydrothermal method has proved to be a promising technique for the preparation of highly stable, infinite metal-ligand frameworks with interesting properties.[2] Two novel complexes of *N*-

(phosphonomethyl)-iminodiacetic acid, $\{H_2O_3PCH_2N(CH_2COOH)_2 (H_4PMIDA)\}$, namely $[Co(PMIDA)(H_2O)_5]\cdot H_2O$, whose structure contains double layers of Co(II) carboxylate interconnected by layers of Co(II) phosphonate and a zinc carboxylate−phosphonate hybrid layered complex, $[Zn_2(PMIDA)(CH_3CO_2H)]\cdot H_2O$, have been recently reported.[3] It has been shown that the deprotonation of the phosphonic ligand has a strong effect on the structure of the metal phosphonates formed. In the previous Co(II) and Zn(II) compounds, the imino nitrogen is not protonated. The reaction of the previous ligand with a zirconium salt in the presence of phosphoric acid produces a mixed phosphate−phosphonate layered compound whereas in the absence of phosphoric acid a linear chain compound is isolated; in both the latter cases, the imino nitrogen is protonated.[4] Wood et al.[5] isolated the canted antiferromagnetic compound $[K_2Co(PMIDA)]_6\cdot xH_2O$, which consists of hexameric

---

* To whom correspondence should be addressed.
† Department of Chemistry.
‡ Department of Physics.

(1) (a) Stein, E.; Clearfield, A.; Subramanian, M. A. *Solid State Ionics* **1996**, *83*, 113. (b) Alberti, G.; Costantino, U. In *Comprehensive Supramolecular Chemistry*; Lehn, J.-M., Ed.; Pergamon-Elsevier Science Ltd.: London, 1996; p 1. (c) Clearfield, A. *Metal Phosphonate Chemistry in Progress in Inorganic Chemistry*; Karlin, K. D., Ed.; John Wiley & Sons: New York, 1998; Vol. 47, pp 371−510, and references therein. (d) Clearfield, A. *Curr. Opin. Solid State Mater. Sci.* **1996**, *1*, 268.

(2) (a) Rujiwatra, A.; Kepert, C. J.; Claridge, J. B.; Rosseinsky, M. J.; Kumagai, H.; Kurmoo, M. *J. Am. Chem. Soc.* **2001**, *123*, 10584. (b) Lin, W. B.; Wang, A. Y.; Ma, L. *J. Am. Chem. Soc.* **1999**, *121*, 11249.

(3) Mao, J. G.; Clearfield, A. *Inorg. Chem.* **2002**, *41*, 2319.

(4) (a) Zhang, B.; Poojary, D. M.; Clearfield, A.; Peng, G. Z. *Chem. Mater.* **1996**, *8*, 1333. (b) Poojary, D. M.; Clearfield, A. *J. Organomet. Chem.* **1996**, *512*, 237. (c) Poojary, D. M.; Zhang, B.; Clearfield, A. *Angew. Chem., Int. Ed. Engl.* **1994**, *33*, 2324. (d) Clearfield, A.; Sharma, C. V. K.; Zhang, B. *Chem. Mater.* **2001**, *13*, 3099. (e) Zhang, B.; Poojary, D. M.; Clearfield, A. *Inorg. Chem.* **1998**, *37*, 249.

(5) Gutschke, S. O. H.; Price, D. J.; Powell, A. K.; Wood, P. T. *Angew. Chem., Int. Ed.* **1999**, *38*, 1088.

rings in the chair conformation and fully deprotonated ligands. A variety of metal phosphonates such as mononuclear chelate complexes, one-dimensional (1-D) chains and three-dimensional (3-D) networks based on dimeric units, and pillared layered compounds may be formed, when two phosphonate groups are attached to a substituted diamine such as $HO_3PCH_2NHRNHCH_2$-PO_3H_2.[6] The crystal structure of copper complex with $C_2H_5N(CH_2PO_3H_2)_2$ was reported by Makaranets et al.[7] and, recently, the *N*-methyliminobis(methylenephosphonic acid) (H_4L) complexes $Mn(H_3L)_2 \cdot H_2O$, $Cd(H_3L)_2 \cdot H_2O$, $Zn_3(HL)_2$, and $Zn(H_2L)(H_2O)$ were reported by our laboratories.[8] The two former isostructural compounds exhibit layered structures, whereas $Zn_3(HL)_2$ and its 1:1 complex $Zn(H_2L)(H_2O)$ form a 3-D network and a double chain, respectively. Herein, we report the hydrothermal syntheses, X-ray structural determinations, and magnetic properties of new types of organophosphonate materials with Cu(II), Co(II), and Mn(II).

Experimental Section

Materials and Methods. The starting materials $Cu(ClO_4)_2 \cdot 6H_2O$, $Co(ClO_4)_2 \cdot 6H_2O$, and iminobis(methylenephosphonic acid) (H_4L) were obtained from Aldrich; H_4L was recrystallized from ethanol. The starting material $MnCl_2 \cdot 4H_2O$ was purchased from Mallinckrodt. The deionized water used was purified with a Barnstead Nanopure II System to a resistivity of 17.6 MΩ cm. Elemental analyses were performed by Robertson-Microlit Laboratories Inc., NJ. Thermogravimetric (TG) analyses were carried out with a TGA Q 500 from TA instruments, at a heating rate of 10 °C/min under an oxygen atmosphere. Infrared (IR) spectra were measured as KBr pellets on a Nicolet Nexus 470 FT-IR spectrometer with spectral resolution of 2.00 cm^{-1}. Magnetic susceptibility and magnetization measurements were carried out on a Quantum Design SQUID magnetometer MPMS-XL. dc magnetic measurements were performed with an applied field of 1000 G in the 2–300 K temperature range. Magnetization data were collected in the −7 to 7 T range starting at zero field at 2 K. Data were corrected for diamagnetic contributions calculated from the Pascal constants.[9]

Syntheses. $Cu_3[NH_2(CH_2PO_3)_2]_2$ (**1**).[10] A quantity of iminobis(methylenephosphonic acid) (H_4L) (0.1 mmol) was neutralized with triethylamine to pH ∼ 6. The neutralized ligand solution was added to 0.1 mmol of $Cu(ClO_4)_2 \cdot 6H_2O$ in 10 mL of deionized water and the mixture was sealed in a 30-mL Teflon-lined autoclave kept at 150 °C for 24 h. Blue cubic crystals of **1** were recovered in ca. 59.3% (0.176 g, based on ligand). Anal. Calcd for $C_4H_{12}N_2O_{12}P_4Cu_3$: C, 8.08%; H, 2.03%; N, 4.71%. Found: C, 8.10%; H, 1.97%; N, 4.59%. IR (KBr pellets): 1627 cm^{-1} {$\delta(NH_2^+)$}; 1097, 1056 cm^{-1} {$\nu_{as}(PO_3)$}; 980 cm^{-1} {$\nu_s(PO_3)$}; 542 cm^{-1} {$\nu(Cu-O)$}.

$Co_3[NH_2(CH_2PO_3)_2]_2$ (**2**). A quantity of iminobis(methylenephosphonic acid) (H_4L) (0.1 mmol) was neutralized with triethylamine to pH ∼ 5. The neutralized ligand solution was added to 0.1 mmol of $Co(ClO_4)_2 \cdot 6H_2O$ in 10 mL of deionized water and the mixture was sealed in a 30-mL Teflon-lined autoclave and kept at 160 °C for 24 h. Purple cubic crystals for **2** were recovered in ca. 12.3% (0.0356 g, based on ligand). Anal. Calcd for $C_4H_{10}N_2O_{12}P_4Co_3$: C, 8.30%; H, 1.74%; N, 4.83%. Found: C, 8.32%; H, 2.02%; N, 4.77%. IR (KBr pellets): 1611s cm^{-1} {$\delta(NH_2^+)$}; 1130, 1013 cm^{-1} {$\nu_{as}(PO_3)$}; 977 cm^{-1} {$\nu_s(PO_3)$}; 555 cm^{-1} {$\nu(Co-O)$}.

$Mn[NH_2(CH_2PO_3H)_2]_2(H_2O)_2$ (**3**). Complex **3** was synthesized by hydrothermal reaction. A quantity of $MnCl_2 \cdot 4H_2O$ (0.1 mmol) and iminobis(methylenephosphonic acid) (H_4L) (0.1 mmol) added to 5 mL of deionized water was sealed into a Teflon-lined autoclave and the pH of the mixture solution was adjusted to ∼3 with triethylamine; the Teflon-lined autoclave was heated at 150 °C for 2 days. Colorless crystals for **3** were recovered in ca. 64.1% (0.16 g). Anal. Calcd for $C_4H_{20}N_2O_{14}P_4$-Mn: C, 9.63%; H, 4.04%; N, 5.61%. Found: C, 9.70%; H, 3.91%; N, 5.54%. IR (KBr pellets): 3498 cm^{-1} {$\nu_s(OH)$}; 1598s cm^{-1} {$\delta(NH_2^+)$}; 1144, 1043 cm^{-1} {$\nu_{as}(PO_3)$}; 940s cm^{-1} {$\nu(POH)$}; 497 cm^{-1} {$\nu(Mn-O)$}.

Single-Crystal X-ray Diffraction Studies. X-ray data sets were collected on a Bruker Smart 1000 CCD equipped with graphite monochromated Mo Kα radiation ($\lambda = 0.71073$ Å) at 110(2) K. The cell constants were indexed from reflections obtained from 60 frames with an exposure time of 10 s/frame. A hemisphere of data (1271 frames at 5-cm detector distances) was collected with scan widths of 0.30° in ω and exposure times of 30, 40, and 30 s/frame for **2** and **3**, respectively. A full sphere of data for **1** was collected. The first 50 frames were recollected at the end of data collection to assess the stability of the crystals; it was found that the decay in intensity was less than 1%. The data sets were corrected for the Lorentz factor, polarization, air absorption, and absorption due to variations in the path length through the detector faceplate.

The space groups were uniquely determined to be *Pbca* (No. 61), $P2_12_12$ (No. 18), and $P2_1/n$ (No. 14) for **1**, **2**, and **3**, respectively. The structures were solved using direct methods (SHELXTL) and refined by least-squares methods with atomic coordinates and anisotropic thermal parameters for all non-hydrogen atoms.[11] All hydrogen atoms were generated geometrically, assigned fixed isotropic thermal parameters, and included in the structure factor calculations. In **1** and **2**, the two highest electron density peaks are located in a special position of the space group. Crystal parameters and information pertaining to data collection and refinement for both structures are summarized in Table 1. Important bonding distances and angles for **1**, **2**, and **3** are listed in Table 2, which is deposited in the Supporting Information. Further crystallographic details as well as atom displacement parameters are also given in the Supporting Information.

Results and Discussion

Syntheses. Reactions of iminobis(methylenephosphonic acid) (H_4L) with the copper and cobalt perchlorate salts, via a hydrothermal reaction, affords two 3:2 (M:L) complexes with 3-D frameworks. Both the perchlorate as well as the chloride salts can be used as starting materials. The lower pH value of the hydrothermal reaction manganese chloride yields a 1:2 layered complex. Scheme 1 shows the ligand H_4L (a) and the different coordination modes it adopts in the manganese (b), copper (c), and cobalt (d) complexes. H_4L is found in the zwitterion form (Scheme 1a), which is the common form for phosphonic acids containing amine groups. Such *N*-methyl-iminobis(methylphosphonic acid) zwitterions are stitched together in 3-D networks by

(6) (a) Song, H. H.; Zheng, L. M.; Wang, Z. M.; Yan, C. H.; Xin, X. Q. *Inorg. Chem.* **2001**, *40*, 5024. (b) Choi, N.; Khan, I.; Matthews, R. W.; McPartlin, M.; Murphy, B. P. *Polyhedron* **1994**, *13*, 847. (c) LaDuca, R.; Rose, D.; DeBord, J. R. D.; Haushalter, R. C. C.; O'Conner J.; Zubieta, J. *J. Solid State Chem.* **1996**, *123*, 408. (d) Soghomonian, V. R.; Diaz, R. C.; Haushalter, C.; O'Conner, J.; Zubieta, J. *Inorg. Chem.* **1995**, *34*, 4460.

(7) Makaranets, B. I.; Polynova, T. N.; Mitrofanova, N. D.; Porai-Koshits, M. A. *J. Struct. Chem.* **1991**, *32*, 94.

(8) (a) Mao, J. G.; Wang, Z. K.; Clearfield, A. *Inorg. Chem.* **2002**, *41*, 2334. (b) Mao, J. G.; Wang, Z. K.; Clearfield, A. *J. Chem. Soc., Dalton. Trans.* **2002**, 4457.

(9) *Theory and Applications of Molecular Paramagnetism*; Boudreaux, E. A., Mulay, L. N., Eds.; John Wiley & Sons: New York, 1976.

(10) Kong, D. Y.; Li, Y.; Ross, J. H., Jr.; Clearfield, A. *Chem. Commun.* **2003**, 1720.

(11) Sheldrick, G. M. *SHELXTL*, version 5.03; Simens Analytical X-ray Instruments: Madison, WI, 1995. Sheldrick, G. M. *SHELX-96 Program for Crystal Structure Determination*; Bruker-AXS: Madison, WI, 1996.

Table 1. Crystallographic Data and Structural Refinement Parameters for $Cu_3[NH_2(CH_2PO_3)_2]_2$ (1), $Co[NH_2(CH_2PO_3)_2]_2$ (2), and $Mn[NH_2(CH_2PO_3H)_2]_2(H_2O)_2$ (3)

molecular formula	$Cu_3[NH_2(CH_2PO_3)_2]_2$	$Co_3[NH_2(CH_2PO_3)_2]_2$	$Mn[NH_2(CH_2PO_3H)_2]_2(H_2O)_2$
formula weight	594.66	580.83	499.04
crystal color	blue, cubic	purple, block	colorless, block
size mm	$0.22 \times 0.15 \times 0.13$	$0.21 \times 0.06 \times 0.02$	$0.28 \times 0.23 \times 0.04$
crystal system	orthorhombic	orthorhombic	monoclinic
a, Å	9.4430(10)	10.7346(8)	7.3668(11)
b, Å	9.3681(10)	13.3704(10)	8.1540(12)
c, Å	16.0755(17)	5.3699(4)	14.090(2)
α, deg	90	90	90
β, deg	90	90	103.935(2)
γ, deg	90	90	90
V, Å³	1422.1(3)	770.72(10)	821.4(2)
space group	*Pbca*	*P2$_1$2$_1$2*	*P2$_1$/n*
Z	4	2	2
D_{calc}, g cm^{-3}	2.777	2.494	2.018
$F(000)$	1172	574	510
θ range, deg	2.53−28.27	1.52−28.29	2.88−28.20
coeff, μ, mm^{-1}	4.968	3.673	1.269
T (K)	110(2)	110(2)	110(2)
λ, Å	0.71073	0.71073	0.71073
reflection collected	7628	1785	9094
independent reflections	1627 (Rint = 0.073)	1761 (Rint = 0.00)	1947 (Rint = 0.022)
completeness to θ	92.4%	94.3%	96.1%
data/restraints/parameter	1627/0/119	1761/0/115	1947/0/155
refine method	full-matrix least squares on F^2	full-matrix least squares on F^2	full-matrix least squares on F^2
R^a and $R_w{}^b$	0.0529; 0.1325	0.0372; 0.0950^c	0.0397; 0.0870
GOF on F^2	1.037	0.983	1.311

^{a} $R = \Sigma||F_o| - |F_c||/\Sigma F_o$. ^{b} $R_w = \{[\Sigma(F_o^2 - F_c^2)^2/[\Sigma w(F_o^2)^2]\}^{1/2}$. ^{c} Based on 10/90 twin, Flack factor is 0.49.

Scheme 1. Ligand H_4L and Its Coordination Modes in Divalent Metal Complexes [Mn(b), Cu(c), Co(d)]

(a)   (b)   (c)   (d)
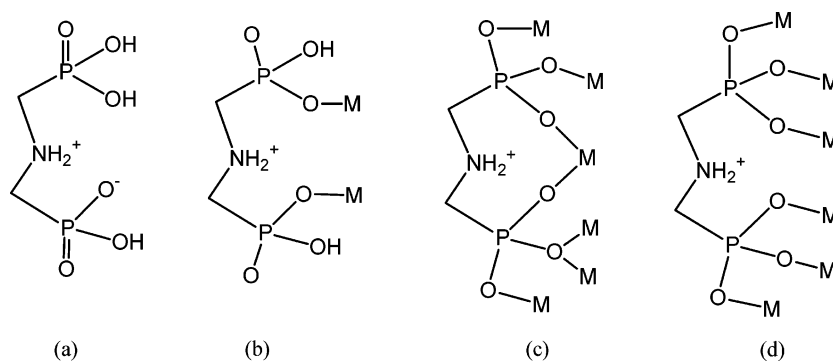
strong hydrogen bonds. Upon reaction with cobalt nitrate in the presence of KOH at room temperature, another proton of the phosphonate group is removed; thus, complexes in a 1:2 ratio (M:L) such as Co-$[NH_2(CH_2PO_3H)_2]_2(H_2O)_2$ [12] and $Mn[NH_2(CH_2PO_3H)_2]_2$-$(H_2O)_2$ are formed. In these compounds, the ligand adopts a bidentate bonding mode to produce 1-D chains, whereas the uncoordinated phosphonate groups are available for intra- and interlayer hydrogen bonding. The latter type of bonding was not observed in our former work with *N*-methyl-iminobis(methylenephosphonic acid).[7,8] Three types of structures have been observed, namely, the layered metal phosphonates $M[NHCH_3(HO_3PCH_2)_2]_2·2H_2O$ (M = Mn, Cd), $Zn[(HO_3$-$PCH_2)(O_3PCH_2)NHCH_3](H_2O)$, with a double-chain structure and $Zn_3[NHCH_3(O_3PCH_2)_2]_2$ with a 3-D network. Under hydrothermal conditions at higher temperature (150 °C), all protons on both phosphonate groups are removed, but the amine group remains protonated. The ligand with three negative charges forms with copper and cobalt perchlorate 3:2 (M:L) complexes, namely, $Cu_3[NH_2(CH_2PO_3)_2]_2$ and $Co_3[NH_2(CH_2PO_3)_2]_2$, and it

provides versatile coordination modes for Cu and Co as depicted in Scheme 1 (c and d). H_4L in the cobalt complex acts as a hexadentate ligand, bridging six Co(II) ions. In the copper complex, the ligand is simultaneously bound η^2-O and μ-O and is bound to six Cu(II) ions in an elaborate structure; at pH 6, the imino nitrogen remains protonated. The deprotonation of the amine group depends on the basicity of the solution, the affinity of the metal ions for the nitrogen atom, and the properties of the chelate rings. Cabeza et al.[13] have reported the same compound, $Cu_3[NH_2(CH_2PO_3)_2]_2$, by the unexpected C−N cleavage reaction after refluxing $CuCl_2$ and nitrilotris(methylene)triphosphonic acid (TPA), $[N(CH_2PO_3H_2)_3]$, in water at pH 2 for 9 days. The structural model has been obtained in the ab initio studies by powder diffraction data. Thus, $Cu_3[NH_2(CH_2$-$PO_3)_2]_2$ can be synthesized from different ligands: either TPA or iminobis(methylenephosphonic acid) via different synthetic routes, reflecting its stability relative to other possible products. As reported for the structure of a Cu(II) complex with ethylaminebis(methylphosphonate), after removal of the amine proton, the nitrogen atom is coordinated to the central Cu(II) atom.[7]

(12) Jankovics, H.; Dashalakis, M. C.; Raptopoulou, P.; Terzis, A.; Tangoulis, V.; Giapintzakis, J.; Kiss, T.; Slifoglou, A. *Inorg. Chem.* **2002**, *41*, 3366.

(13) Cabeza, A.; Bruque, S.; Guagliardi, A.; Aranda, M. A. G. *J. Solid State Chem.* **2001**, *160*, 278.
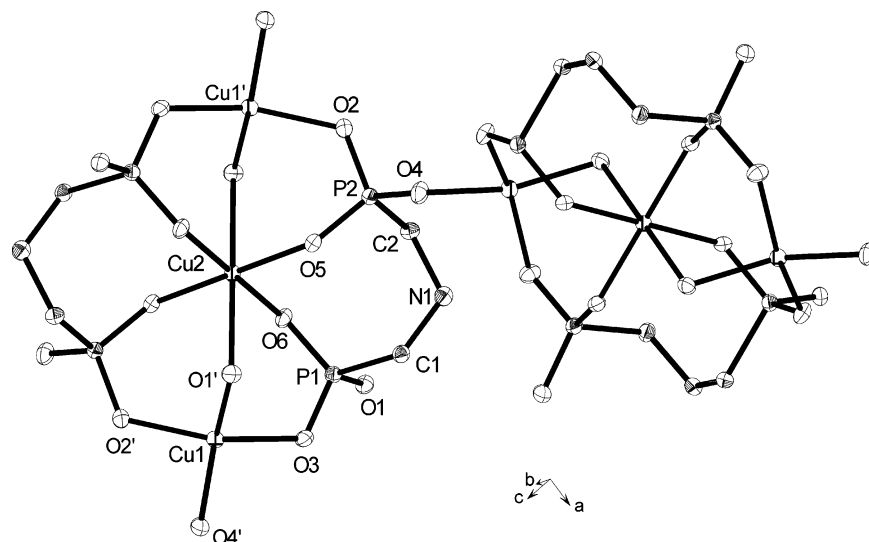
Figure 1. ORTEP representation of compound **1** at the 50% probability level along with the atom-labeling scheme.
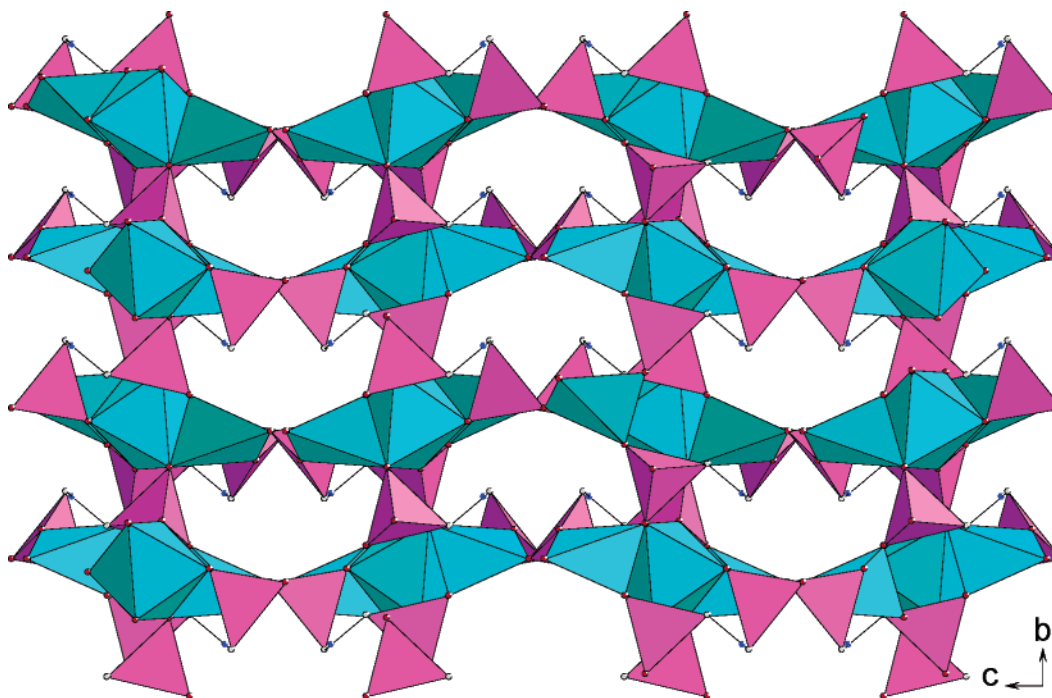

Figure 2. View of the crystal structure of compound **1** along the *a* axis. The phosphonate groups $C-PO_3$ and Cu_2O_9 are represented by tetrahedra (purple) and polyhedra (cyan). N and P atoms are shown as light gray circles and black solid circles, respectively.

The FT-IR spectra of complexes **1**, **2**, and **3** exhibit intense absorptions at 1627, 1611, and 1598 cm^{-1}, respectively, assigned to $\delta(NH_2)^+$. Additionally, two types of $\nu_{as}(PO_3)$ are inferred from the presence of peaks at 1097 and 1056, 1130 and 1013, and 1144 and 1043 cm^{-1}, for compounds **1**, **2**, and **3**, respectively.[14] Symmetric stretching vibrations $\nu_s(PO_3)$ were observed at 980 and 977 cm^{-1} for **1** and **2**, respectively. The sharp feature at 940 cm^{-1} observed for compound **3** is assigned to $\nu(POH)$ mode. No such bands were observed in the former two compounds. These observations are consistent with the X-ray structural analysis (vide supra). The aforementioned stretching vibrations are shifted to lower values compared to those of the free ligand,

indicating coordination of the latter to the metal ions. The metal–ligand (M–O) strectching vibrations are located at ~542, 555, and 497 cm^{-1} for **1**, **2**, and **3**, respectively. The coordinated water stretching vibration ($\nu_s(OH)$) for **3** appears at 3498 cm^{-1} and is absent in the FT-IR spectra of **1** and **2**.

Thermal Analyses. TG measurements of **1** indicate that combustion of the organic ligand begins at 300 °C and continues in several steps to 1000 °C. The TGA diagram of complex **2** is simple with a single weight loss step that continues to 1000 °C. The final products are mainly $Co_2P_2O_7$; the calculated weight loss (26.39%) is slightly higher than that observed (25.16%), and thus the reaction is not complete at 1000 °C as evidenced by the fact that the weight is still decreasing at that temperature. The TGA diagram of complex **3** shows two major weight loss steps. The first step is completed at

(14) (a) Corbridge, D. E. C. *J. Appl. Chem.* **1956**, *6*, 456. (b) Gore, R. C. *Discuss. Faraday Soc.* **1950**, *9*, 138. (c) Thomas, L. C.; Chittenden, R. A. *Spectrochim. Acta* **1964**, *20*, 467.
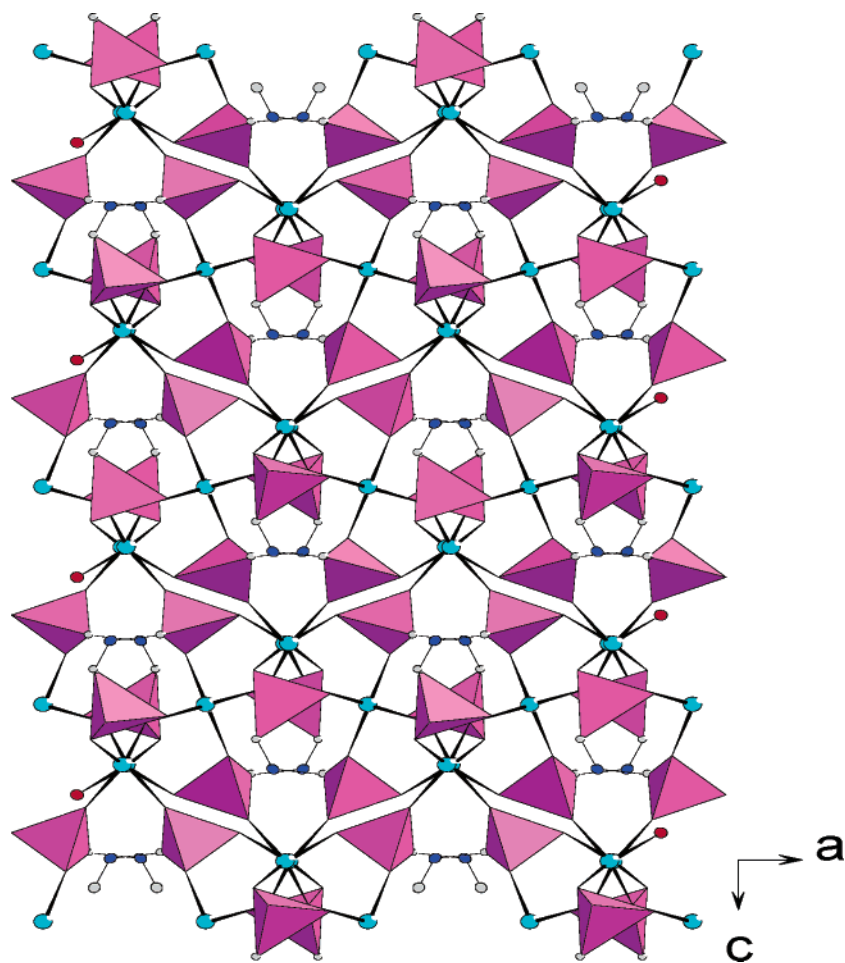
Figure 3. View of crystal structure of compound **1** along the *b* axis. The phosphonate groups C−PO$_3$ are represented by tetrahedra (purple). Cu, N, P, and C atoms are shown as cyan, blue, red, and gray solid circles.
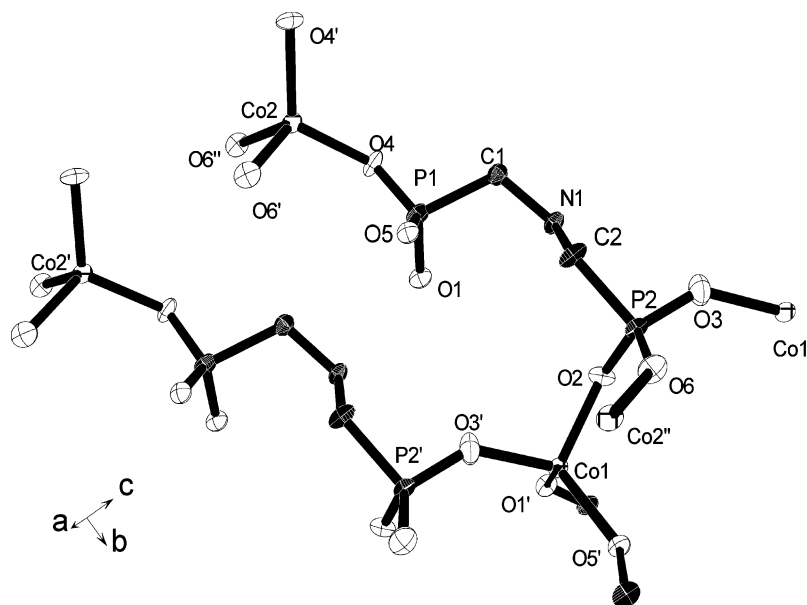

Figure 4. ORTEP representation of compound **2** at the 50% probability level with the atom-labeling scheme.

230 °C. The observed weight loss (8.00%) is in good agreement with the calculated value (7.22%) for the loss of two coordinated water molecules. There are two processes taking place between 300 and 600 °C, namely, the release of two water molecules formed by the condensation of hydrogen phosphonate groups and the pyrolysis of the organic group. The weight loss stops

after 950 °C. The final product is the metaphosphate Mn(PO$_3$)$_2$, and the calculated weight loss (57.34%) is in agreement with that observed (57.13%).

Crystal Structures. *Cu$_3$[NH$_2$(CH$_2$PO$_3$)$_2$]$_2$ (**1**).* The X-ray crystallographic determination of compound **1** reveals two different Cu coordination environments, namely, distorted square planar and octahedral Cu(II)
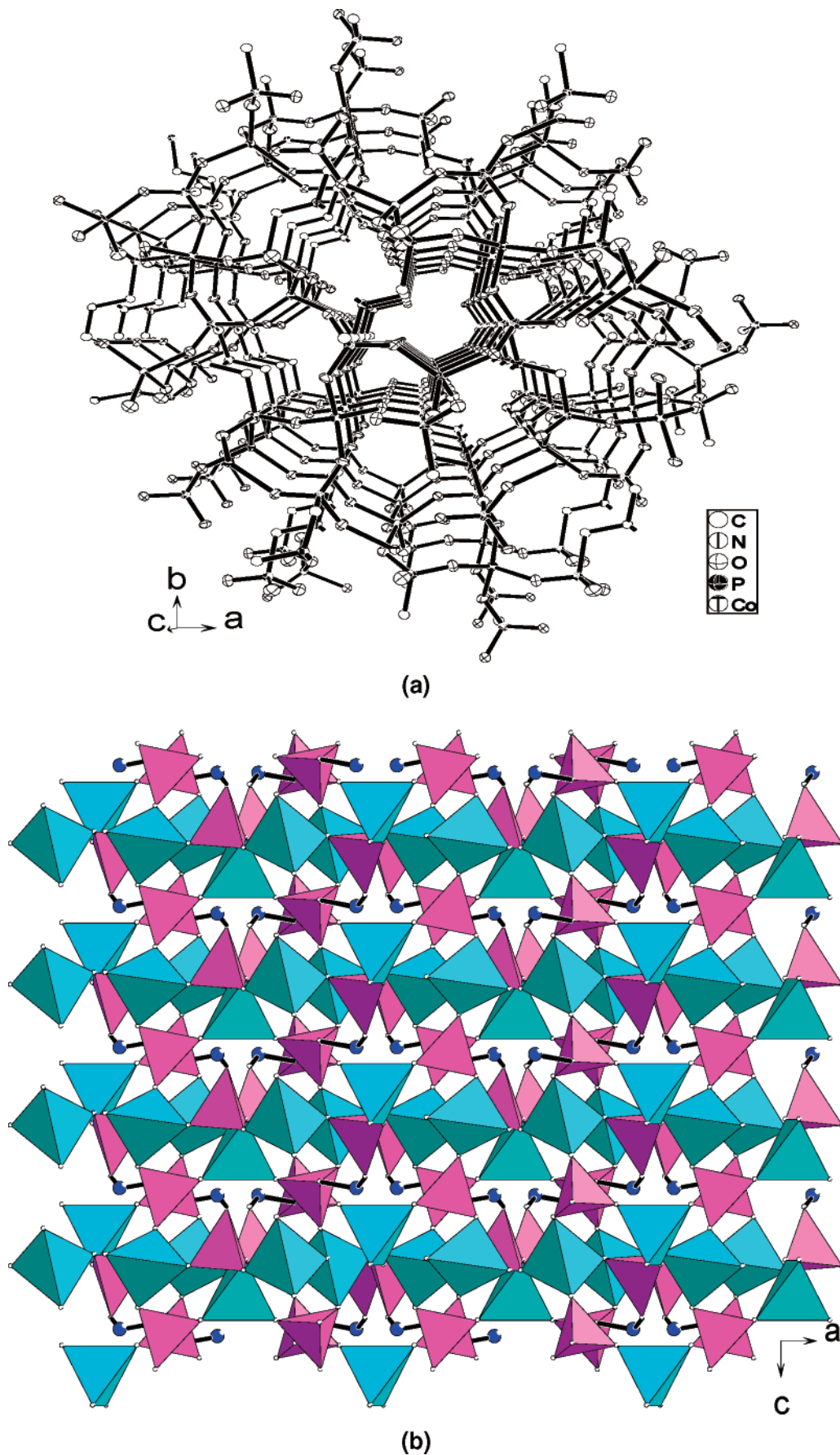
(a)

(b)

Figure 5. (a) A view of compound **2** along the *c* axis. (b) View of compound **2** in the *ac* plane. The phosphonate groups $C-PO_3$ and $Co-O_4$ are represented by purple and cyan tetrahedra, respectively. N atoms are shown as blue spheres.

ions that are bridged by an oxygen atom to form a local trimeric unit, which are further connected into a 3-D framework of corner-sharing layers (Figure 1). Both hexadentate phosphonate groups are fully deprotonated, whereas the amine group remains protonated. The protonated nitrogen atoms form hydrogen bonds with phosphonate oxygen atoms {N(1)−H(1D)···O(5) 2.720 (5) Å, 173(4)°}. The Cu_2O_9 polyhedra are interconnected by phosphonate groups, resulting in the formation of 3-D networks that include interstitial spaces (Figure 2). Three copper ions and two ligand molecules form 16-membered rings as shown in Figure 1. An octahedral copper ion (Cu2) is located in the center of the 16-membered ring and is connected with the other two distorted square planar copper atoms through two equivalent bridged phosphonate oxygen atoms (O1, O1′). The adjacent 16-membered rings are tilted away from each other in corner-sharing layers to form a 3-D framework. Each 16-membered ring has a center of symmetry with the octahedral copper ions located at the inversion center. There are two different bond distances between the bridging O(1) atom and the Cu(1) and Cu-(2) [Cu(1)−O(1) = 1.929(3) Å, Cu(2)−O(1) = 2.389(3) Å compared with the powder structure: 1.958(14) and 2.418(12) Å, respectively[13]]. The elongated bond distances are assigned to a typical Cu(II) ion in a Jahn−Teller distortion, while the shorter bond distance is normal for equatorial 4-coordinated Cu−O bonds. Hydrogen bonds are formed between the protonated amine groups and each phosphonate oxygen atom {N1−H1B···O1 2.720 Å 173.30°}.

$Co_3[NH_2(CH_2PO_3)_2]_2$ (**2**). The structure of **2** differs from that of **1**, although both compounds form 3-D networks. The asymmetric unit of **2** consists of three cobalt atoms and two ligand molecules. All the Co(II) ions are surrounded by oxygen atoms in a tetrahedral environment, with each ligand bound to adjacent Co(II) ions. (Figure 4) The Co−O distances range from 1.927-(6) to 1.982(5) Å, which are similar to the 3-D metal-organic framework with bridging L−H_2 (L = 2,2′-diethoxy-1,1′-binaphthalene-6,6′-bisphosphonic acid) groups and both six- and four-coordinated Co(II) centers reported by Lin et al.[15] In $[Co_2(L−H_2)(H_2O)_3](H_2O)_4$, the tetrahedral Co(II) center has bond distances that range from 1.935(1) to 1.974(1) Å. The Co−O bond distances of complex **2** are slightly shorter than those of its analogue $Co[NH_2(CH_2PO_3H)_2]_2(H_2O)_2$ (2.067(2), 2.132(2) Å) which features a 1-D chain layered structure in which the cobalt atoms are found in a distorted octahedral environment.[12] The Co−O distances in **2** are shorter than those in the other phosphonate derivatives [2.104(4)−2.121(4) and 2.053(2)−2.107(2) Å for $Co(NH_3CH_2PO_3)_2(H_2O)_2]_n·nH_2O$ and $Co_2[O_3PCH_2N(CH_2COO)_2](H_2O)_5]·H_2O$, respectively]. A twisted 12-membered ring of Co1, O6, P1, C1, N1, C2, P2, O8, Co2, O4, P1, and O1 is interconnected with an eight-membered ring which contains Co2, O8, P2, O2, Co1, O6, P1, and O4 by sharing PO_4 polyhedra as shown in Figure 5a. The distances between Co1···Co2, Co2···Co2, and Co1···Co1 are 3.910, 5.370, 7.539 Å, respectively. The ring size is larger than the copper 16-membered ring in which the bond distances between two adjacent metal atoms are Cu1···Cu2 = 3.344 Å and Cu1···Cu1 = 6.689
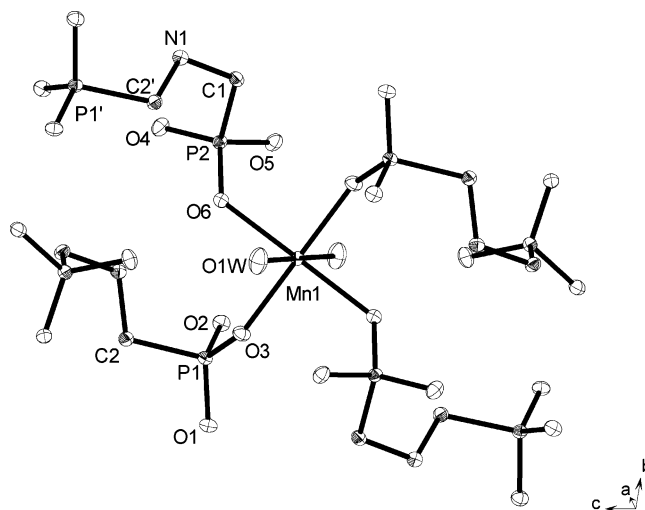
(15) Evans, O. R.; Manke, D.; Lin, W. *Chem. Mater.* **2002**, *14*, 3866.

Figure 6. ORTEP representation of compound **3** at the 50% probability level with the atom-labeling scheme.

Å. Hydrogen bonds are formed between the protonated amine groups and two phosphonate oxygen atoms {N1−H1B···O1 2.744 Å, 153.79°}.

A high residue peak (6.9 e/Å³) was located in the final Fourier map, the existence of which suggested the existence of an intergrowth or a twinned structure. The structure was ultimately modeled as a pair of racemic twins and the twinning ratio was refined as 50/50. To model the microtwin, occupancy numbers of the atoms across the pseudo-mirror plane were refined, and an extra disordered fragment was used to model the residual electronic density. The disorder ratio was refined to 90/10, and the disordered fragment was related to the major fragment by a pseudo mirror plane perpendicular to c (Flack factor of 0.49). With this refinement the R factors were reduced by 50% and the residual electron density was reduced from 6.9 to 0.7 e/Å³. (See Supporting Information for the twin model.)

$Mn[NH_2(CH_2PO_3H)_2]_2(H_2O)_2$ (**3**). Figure 6 depicts the ORTEP diagram along with the atom-labeling scheme for complex **3**. Four phosphonate oxygen atoms and two equivalent water molecules are coordinated to mononuclear octahedral Mn(II) ions. The angles within the equatorial plane defined by O6, O6′, O1w, and O1w′ are in the range 93.67(9)−86.33(9)°. The four ligand molecules which surround the central manganese atom are also coordinated to four other manganese atoms as a consequence of the presence of the second phosphonate group in each molecule. This connectivity extends to form infinite 1-D chains along the b-axis as shown in Figure 7. The two phosphonate oxygen atoms O(2) and O(5) are still protonated as indicated by the longer bond lengths {P(1)−O(2) 1.560(2) Å, P(2)−O(5) 1.559(2) Å} compared to the other four P−O bond lengths {P(1)−O(1) 1.507(2) Å, P(1)−O(3) 1.492(2) Å, P(2)−O(4) 1.505(2) Å, P(2)−O(6) 1.502(2) Å}.

Hydrogen bonds are formed between the protonated phosphonate oxygen and coordinated water oxygen atoms within a layer. {O1w−H1wB···O2 3.079 Å (140.0°), O1w−H1wA···O4#1 2.851 Å (169.0°), O2−H2C···O4#2 2.551 Å (173.0°), O5−H5A···O1#3 2.535 Å (175.0°)}. The 1-D metal phosphonate chains are connected by hydrogen bonds into layers and are further linked by inter-
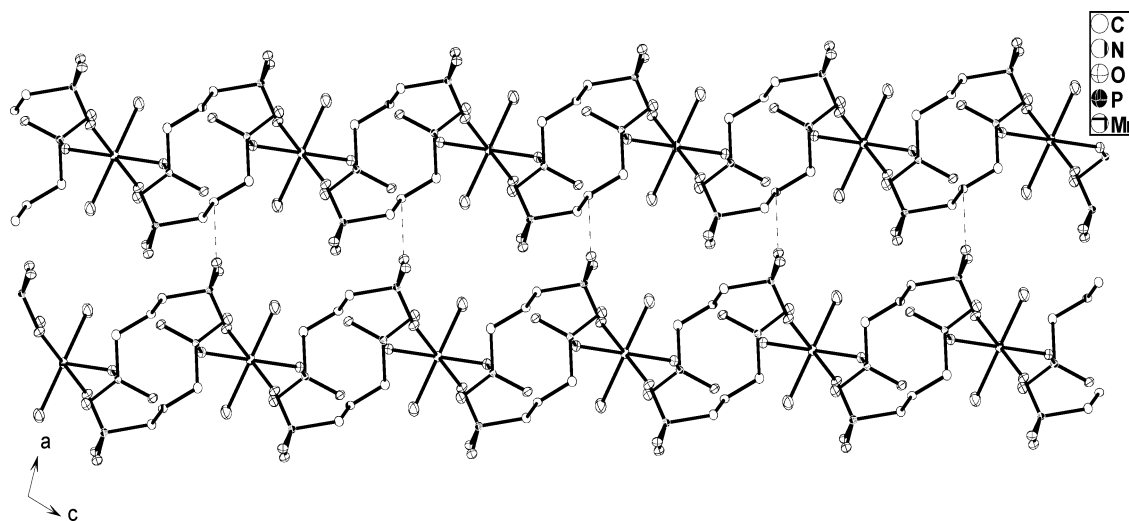
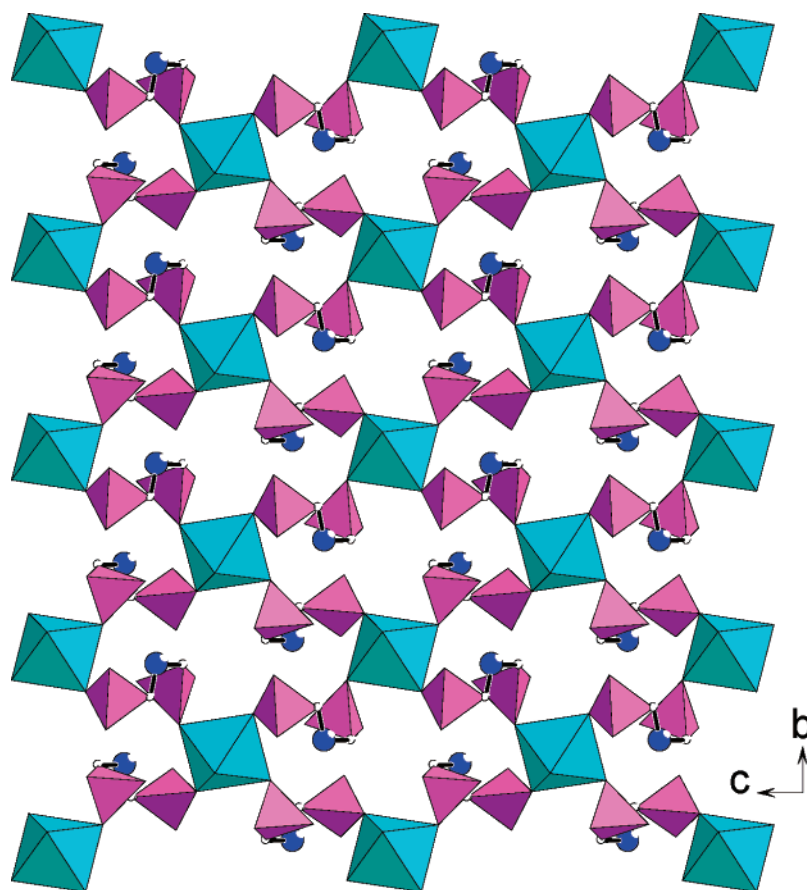**Figure 7.** 1D layered complexes of **3** viewed along the *b* axis.

Figure 8. View of crystal structure of compound **3** down the *a* axis. The phosphonate groups C−PO$_3$ and MnO$_6$ are represented by a purple tetrahedron and cyan octahedron, respectively. N atoms are shown as blue circles.

layer hydrogen bonding between protonated amino groups and the coordinated phosphonate oxygen atom N1−H1D···O6 2.835 Å (156.0°) as shown in Figure 7. Strong hydrogen bonds have been found in similar ligand *N*-methyliminobis(methylenephosphonic acid) and its layered complexes Mn(H$_3$L)$_2$·2H$_2$O, as well as phosphonic acids attached to aza-crown ethers, resulting in the formation of "macroleaflets".[16] The distance between two adjacent intralayered manganese atoms which is bridged by the same ligand is 8.205 Å. In contrast, two interlayered manganese atoms have a shorter contact of 7.367 Å.

Magnetic Properties. Magnetic susceptibility measurements of complexes **1**−**3** were performed on polycrystalline samples of the compound at 1000 Oe over the temperature range 2−300 K. These results are shown in Figures 9−14

Cu$_3$[NH$_2$(CH$_2$PO$_3$)$_2$]$_2$ (1). The value of χT at 300 K is 1.35 emu mol^{-1} K for compound **1**, which is higher than

(16) (a) Matczak-Jon, E.; Kurzak, B.; Kamecka, A.; Sawka-Dbrowolska, W.; Kafarski, P. *J. Chem. Soc., Dalton Trans.* **1999**, 3627. (b) Daly, J. J.; Wheatley, J. *J. Chem. Soc., A* **1967**, 212. (c) Makaranets, B. I.; Polynova, T. N.; Bel'sklii, V. K.; Il'ichev, S. A.; Porai-Koshits, M. A. *J. Struct. Chem.* **1985**, *26*, 761.
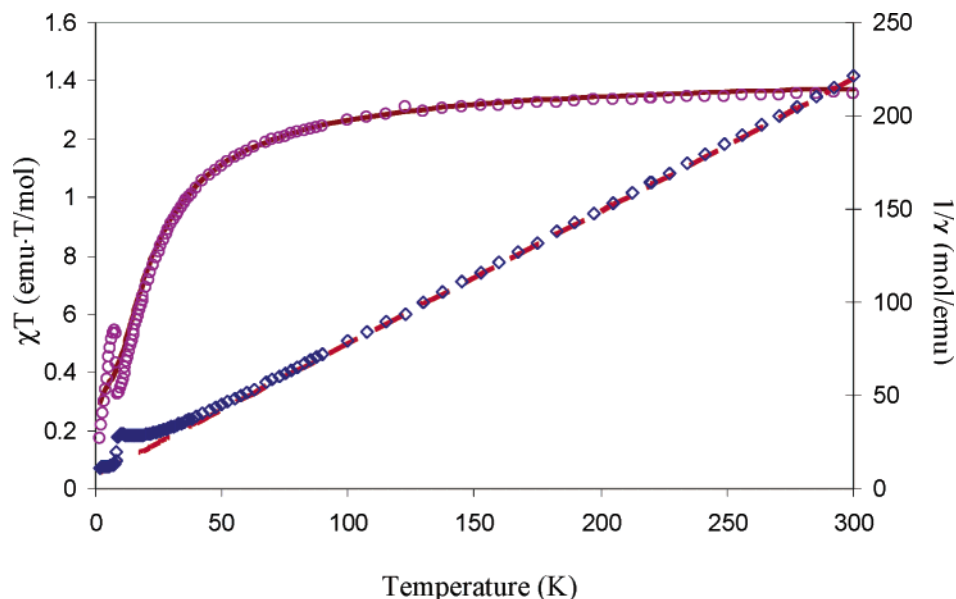
Figure 9. Temperature dependence of the χT product ($\bigcirc$) and the inverse susceptibility ($\Diamond$); solid line corresponds to the best fit obtained with eq 2 and the dashed line the Curie–Weiss law.
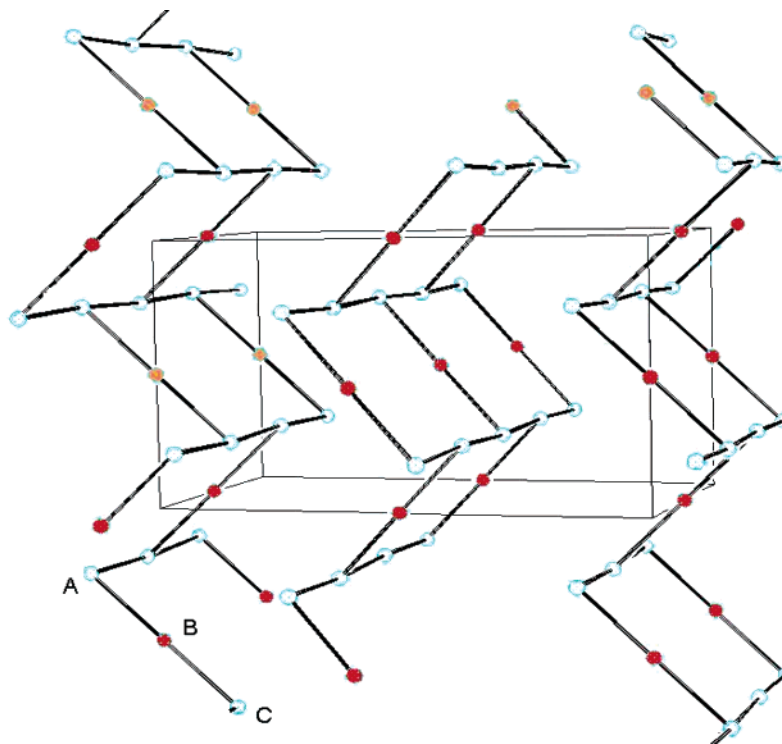

Figure 10. Plot of local magnetic pathways for different Cu atoms. The structure forms a zigzag stacking of the Cu_3 chains. The center of the chain is an octahedral Cu 3.344A to its two terminal neighbors. A tetrahedral Cu is at the end of the chains and is only 4.685A to two Cu atoms from neighboring stacks. The connectivity of the material implies that bonding within the linear three-atom Cu cluster should dominate the magnetic properties, with intercluster magnetic interactions assumed weaker.

the expected spin-only value ($3\chi_{Cu}T = 1.125$ cm^3 mol^{-1} K, $S = {}^{1}/_{2}$), indicating that an important orbital contribution is involved. The χT value continuously decreases from room temperature and reaches a minimum of 0.33 emu mol^{-1} K at 9 K. Below 9 K, χT increases abruptly to reach a maximum at ~7.5 K ($\chi T_{max} = 0.55$ emu mol^{-1} K) and finally decreases again at lower temperatures. The temperature dependence of $1/\chi$ between 300 and 20 K approximates Curie–Weiss behavior with $C = 1.41$ emu mol^{-1} K and $\theta = -10.6$ K. The negative sign of the Curie–Weiss constant indicates antiferromagnetic interactions between Cu(II) centers. (See Figure 9.)

To explain the magnetic interaction among different Cu ions, the local magnetic pathways for these two kinds of Cu(II) sites must be considered. The connectivity of the material dictates that bonding within the Cu trimers formed by bridging oxygen interactions will dominate the magnetic properties, with much weaker coupling between the trimers through bridging phosphonate groups. A simplified stick diagram of the Cu atoms and their connectivities is depicted in Figure 10.

A simple isotropic model nicely describes the magnetic behavior above about 10 K: the model considers the atoms in one trimeric unit A–B–C (as shown in Figure
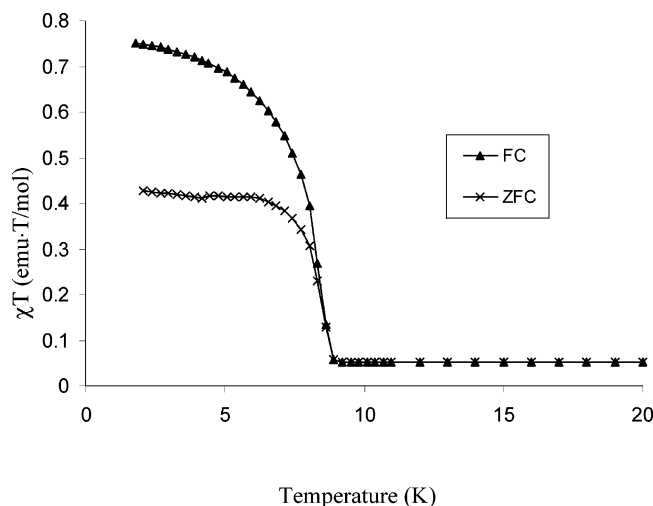
Cu(II), Co(II), and Mn(II) Organophosphonates

Chem. Mater., Vol. 16, No. 16, 2004   **3029**

Figure 11. Temperature dependence of molar susceptibility in the zero-field-cooling and field-cooling for **1**. A divergence of χ_{ZFC} and χ_{FC} started at 8.6 K and became more pronounced at lower temperature. Combining with the measurement of *ac* susceptibility, this irreversibility is attributed to a ferromagnetic transition.
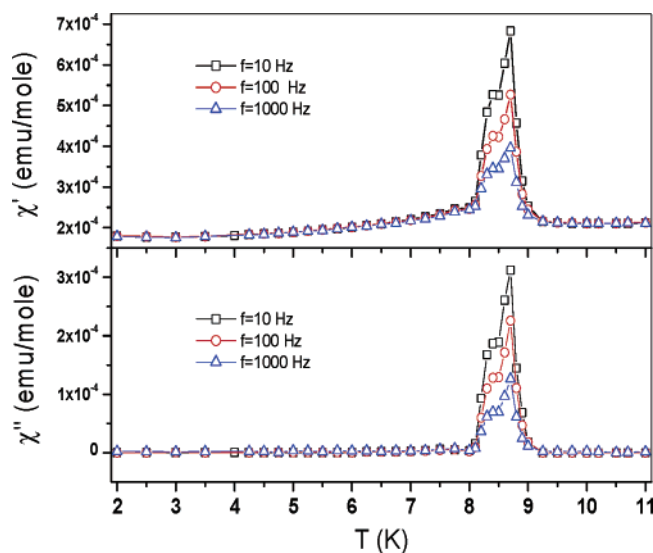

Figure 12. ac susceptibility measured in zero dc and 6 Oe ac field for **1**. Frequencies increase from top to bottom as shown, and there is a peak at 8.7 K and a shoulder at 8.4 K for both χ' and χ''.

10) with the central Cu(II) atom denoted Cu_B, The Hamiltonian, $H = -J(S_A.S_B + S_B.S_C)$ describes the interactions of the three $S = ^1/_2$ Cu centers and gives two $S = ^1/_2$ and one $S = -^3/_2$ state. Assuming $S_A = S_C$, it is straightforward to write the analytical expression for χT vs T according to the usual thermal population of states:

$$\chi T = \frac{N\beta^2}{4k}[((4g_A - g_B)/3)^2 + g_B \exp(J/kT) +$$
$$10((2g_A + g_B)/3)^2 \exp(3J/2kT)]/[1 + \exp(J/kT) + 2\exp(3J/2kT)] \quad (1)$$

Due to weak magnetic interactions between the individual trimeric magnetic units in 3-D, the expression in eq 1 was corrected using the molecular field approximation (eq 2) where χ is the experimental exchange coupled magnetic susceptibility, χ_{Cu} is the magnetic
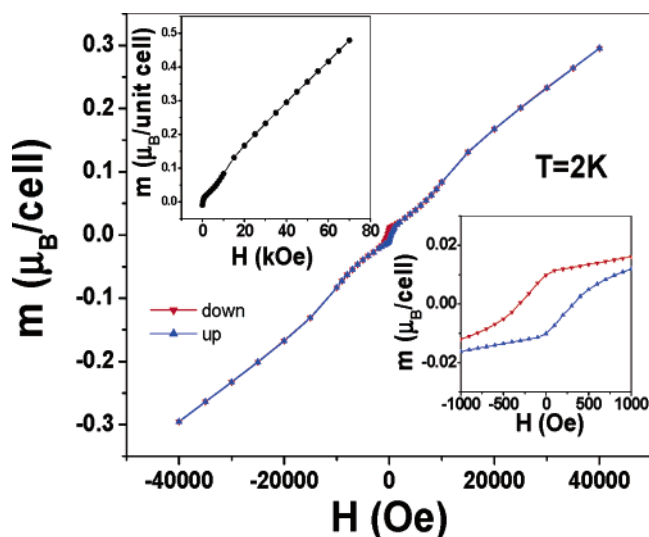

Figure 13. Magnetic hysteresis loop of **1** at 2 K. Magnetic field dependencies of the moment $m(H)$ with field decreasing and increasing are labeled here as "▽" and "△" respectively. Inset right: the details of the M−H loop observed under low field. The coercivity reaches 500 Oe. Insert left: there is no magnetic saturation until 70 kOe.

susceptibility of the Cu trimer, zJ is the exchange parameter, and the other symbols have their usual meanings.[20]

$$\chi = \frac{\chi_{Cu}}{1 - (zJ/Ng^2\beta^2)\chi_{Cu}} \quad (2)$$

The magnetic data were fit to eq 2 in the temperature range of 9−300 K with the parameters $J = -19$ cm^{-1}, $g_A = 2.18$, $g_B = 2.4$, and $zJ = -2$ cm^{-1}.

The observed increase in χT below 9 K corresponds to a weak ferromagnetic ordering at low temperatures due to spin canting of the antiferromagnetically coupled trimer units. The ordering was verified by comparing the zero-field-cooled (ZFC) susceptibility of compound **1** to the data obtained on a field-cooled (FC) sample. Figure 11 depicts the dc molar susceptibility $\chi_{m(ZFC)}$ and $\chi_{m(FC)}$ recorded in zero-field and an applied field $H = 100$ Oe. The divergence of dc χ_{ZFC} and χ_{FC} reveals the history dependence of the magnetization process. Above 8.6 K the magnetization is reversible and behaves similarly for both FC and ZFC samples. To further verify the magnetic transition, ac-susceptibility measurements were performed under a 6 Oe ac field, with the results shown in Figure 12. Both χ'' and χ' signals show a peak located at 8.7 K. No frequency dependence of the ac signals was observed. The observation of magnetic hysteresis at low temperature also supports the onset of an ordering (Figure 13). As shown in the inset of Figure 13, the coercivity is very small at 500 Oe.

(17) Earnshaw, A. *Introduction to Magnetochemistry*; Academic Press: New York, 1968.
(18) (a) Ashcroft, N. W.; Mermin, N. D. *Solid State Physics*; Holt, Rinehart and Winston: New York, 1976; p 699. (b) Mydosh, J. A. *Spin Glasses: An Experimental Introduction*; Taylor and Francis: London, 1993. (c) Li, Y.; Ross, J. H., Jr. *Appl. Phys. Lett.* **2003**, *83*, 2868. (d) Binder, K.; Young, A. P. *Rev. Mod. Phys.* **1986**, *58*, 801.
(19) Mabbs, F. E.; Machin, D. J. *Magnetism and Transition Metal Complexes*; Chapman and Hall: London, 1973; pp 99−100.
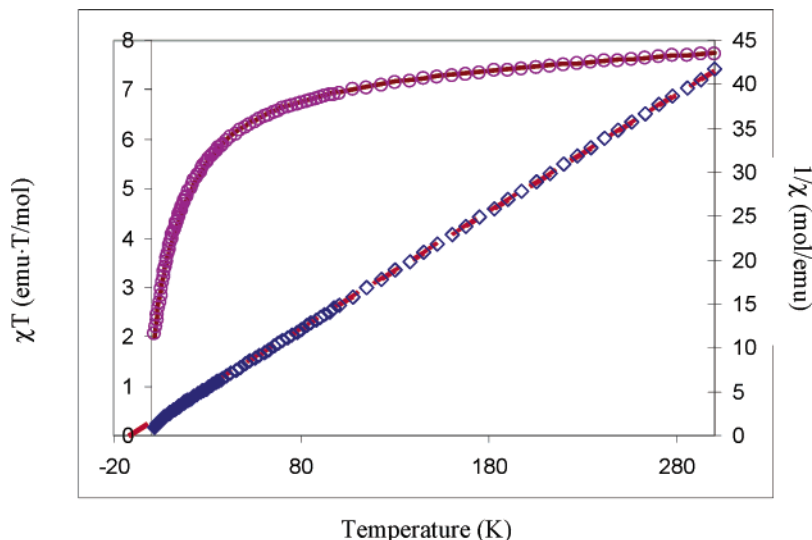(20) Kahn, O. *Molecular Magnetism*; VCH: New York, 1993.

Figure 14. Temperature dependence of the χT product (○) and the inverse susceptibility (◇) for compound **3**. The solid line corresponds to the best fit obtained with eq 2 and the dashed line is a fit to the Curie−Weiss law.

Magnetization measurements at high field performed at 2 K revealed an abrupt increase of the magnetic moment at low fields with a steady increase to a value of 0.5 μ_B at 70 kOe (insert right of Figure 13). No saturation was observed.

$Co_3[NH_2(CH_2PO_3)_2]_2$ (**2**). A plot of the χT versus T dc susceptibility data for compound **2** is shown in Figure 14. The value of χT at 300 K is 7.7 emu mol^{-1} K is higher than the expected spin-only value ($3\chi_{Co}T = 5.625$ cm^3 mol^{-1} K, $S = {}^3/_2$), indicating that an important orbital contribution is involved. The χT values remain nearly constant until ∼80 K, after which there is a smooth decrease at low temperatures. The temperature dependence of $1/\chi$ between 300 and 7 K approximates Curie−Weiss behavior with $C = 7.5$ emu mol^{-1} K and $\theta = -12$ K. The negative sign of the Curie−Weiss constant indicates antiferromagnetic and/or zero-field splitting effects, both of which dominate at low temperature.[19]

The modeling of the magnetic behavior of **2** was carried out with a treatment of the considerable zero-field splitting operative in Co(II) systems. The presence of a ligand-field component of symmetry lower than cubic can cause the magnetic moment to vary with T, as the spin degeneracy of the $^4A_2$ ground state is then lifted. For a d^7 ion in a tetrahedral environment, the first excited state is $^4T_2$ arising from the ^4F free-ion ground state. Under a tetragonal distortion, this state is split into an orbital singlet, $^4B_2$, and an orbital doublet, ^4E. The quartet spin ground state, $^4A_2$, is removed by the combined action of the spin−orbit interaction and the tetragonal crystal field, leading to two Kramers doublets (zero-field splitting). Formally, this behavior can be treated as an $S = {}^3/_2$ spin state under the action of the spin Hamiltonian $H = D[S_z^2 - 1/3 S(S+1)] + g_{||}\beta H_z S_z + g_\perp\beta(H_x S_x + H_y S_y)$, where DS_z^2 represents the splitting into two Kramers doublets in the absence of a magnetic field. In the present notation, positive D values stabilize the $\pm^1/_2$ state. The expression of the magnetic susceptibility is easily derived from the aforementioned Hamiltonian,[20] the parameters involved having their usual meaning.

$$\chi_{Co} = (\chi_{||} + 2\chi_\perp)/3 + TIP \qquad (3)$$

where

$$\chi_{||} = \frac{N\beta^2 g_{||}^2}{4kT}\frac{1 + 9\exp(-D/kT)}{1 + \exp(-D/kT)}$$

and

$$\chi_\perp = \frac{N\beta^2 g_\perp^2}{4kT}\frac{4 + 6kT/D\cdot[1 - \exp(-D/kT)]}{1 + \exp(-D/kT)}$$

The expression in eq 3 was further modified to account for the magnetic exchange interactions (eq 2).

A least-squares fitting of the data using this model leads to $D = 17$ cm^{-1}, $g_{||} = 2.8$, and $g_\perp = 2.0$. Similar values of $|D|$ have already been reported for other tetrahedrally distorted cobalt(II) complexes.[21,22] The temperature-independent paramagnetism (TIP) is 600 × 10^{-6} emu mol^{-1}. The value of $zJ = -0.5$ cm^{-1} indicates that antiferromagnetic exchange between cobalt(II) ions is very weak. It should be noted that the quality of the fit is very good even at low temperatures.

The temperature-dependent magnetic susceptibility for compound **3** indicates that the Mn(II) ions are isolated paramagnets. The data were fit to the Curie law, with $C = 4.4$ emu K mol^{-1}, in good agreement with the expected value for isolated high-spin Mn ions ($S = {}^5/_2$) in a magnetically dilute sample. Considering that the intra- and interlayer Mn---Mn distances are very long (7 Å), it is not surprising that there is no observed coupling between these magnetic centers.

(21) Nelson, D.; Haar, L. W. *Inorg. Chem.* **1993**, *32*, 182.
(22) Duran, N.; Clegg, W.; Cucurull-Sanchez, L.; Coxall, R. A.; Jimenez, H. R.; Moratal, J.-M.; Llret, F.; Gonzalez-Duarte, P. *Inorg. Chem.* **2000**, *39*, 4821.

Cu(II), Co(II), and Mn(II) Organophosphonates

Chem. Mater., Vol. 16, No. 16, 2004 **3031**